PHOTODESTRUCTION CROSS SECTIONS FOR MASS-SELECTED ION CLUSTERS: $(CO_2)_n^+$

M.A. JOHNSON, M.L. ALEXANDER and W.C. LINEBERGER

Department of Chemistry, University of Colorado and Joint Institute for Laboratory Astrophysics, University of Colorado and National Bureau of Standards, Boulder, Colorado 80309, USA

The relative photodestruction cross sections for CO_2 cluster ions, $(CO_2)_n^+$ ($2 \leqslant n \leqslant 10$), are reported at 1064, 644 and 532 nm. The ion clusters are synthesized by nucleation to the monomer ion in a supersonic expansion, and the parent ions are mass selected both before and after photodissociation with a tandem time-of-flight mass spectrometer. Models for the observed cluster size dependence of the cross sections are discussed.

1. Introduction

Interest in the properties of small molecular clusters has been increasing since, in principle, they afford the possibility of incrementally approaching true condensed phase behavior beginning with isolated gas phase species [1]. While conceptually appealing, this goal has been hampered by the difficulty inherent in isolating experimental measurables (that result from a *single* well-characterized cluster) from the distribution of clusters created in typical experiments on neutrals.

While much work has been done on the distribution of cluster sizes formed under various conditions [2—4], the spectroscopic properties of a single, specific, relatively large (e.g. 10 monomer units) clusters have not yet been amenable to direct study. One obvious solution is to study the properties of ionic clusters in the gas phase, but the low densities achievable have prevented the study of all but the smallest cluster ions (e.g. $CO_3^- \cdot (H_2O)_3$ [5] and $(NO)_3^+$ [6]). To overcome this problem, we have constructed a new apparatus which produces ion clusters of light molecular gases (CO_2, N_2, NO, CO, SF_6, etc.) by successive nucleation onto a monomer ion *during* a free-jet expansion [7], mass selects the parent clusters prior to interaction with a photodissociation laser, and finally mass analyzes the fragment ions formed in the photodissociation process.

In this paper we report the first results obtained from this apparatus and present the photodestruction cross sections for $(CO_2)_n^+$, $n = 2-10$, at 532, 644 and 1064 nm. All of the clusters have a non-zero absorption cross section at all wavelengths studied, but the cross section is cluster-size dependent at the two longer wavelengths. Generally, the photodestruction cross sections of the higher clusters mimic the behavior of the dimer, measured previously by Smith et al. [8]. Systematic deviations from the dimer cross section at higher cluster sizes may reflect dynamical behavior of the energized ion or may result from true changes in the absorption cross section owing to the environment of the chromophore at each cluster size.

2. Experimental

A schematic diagram of our tandem time-of-flight apparatus is given in fig. 1. To avoid complications involving internal excitation of ion clusters formed by ionization of neutral clusters [9], we have developed a method of synthesizing the ion clusters by nucleating them onto the monomer ion via clustering reactions occurring during the free-jet expansion. After these collisions have ceased, the clusters are allowed to drift 10 cm in a field-free region and then pulse-ejected from the molecular beam into the first flight tube for mass selection of the parent clusters. The TOF
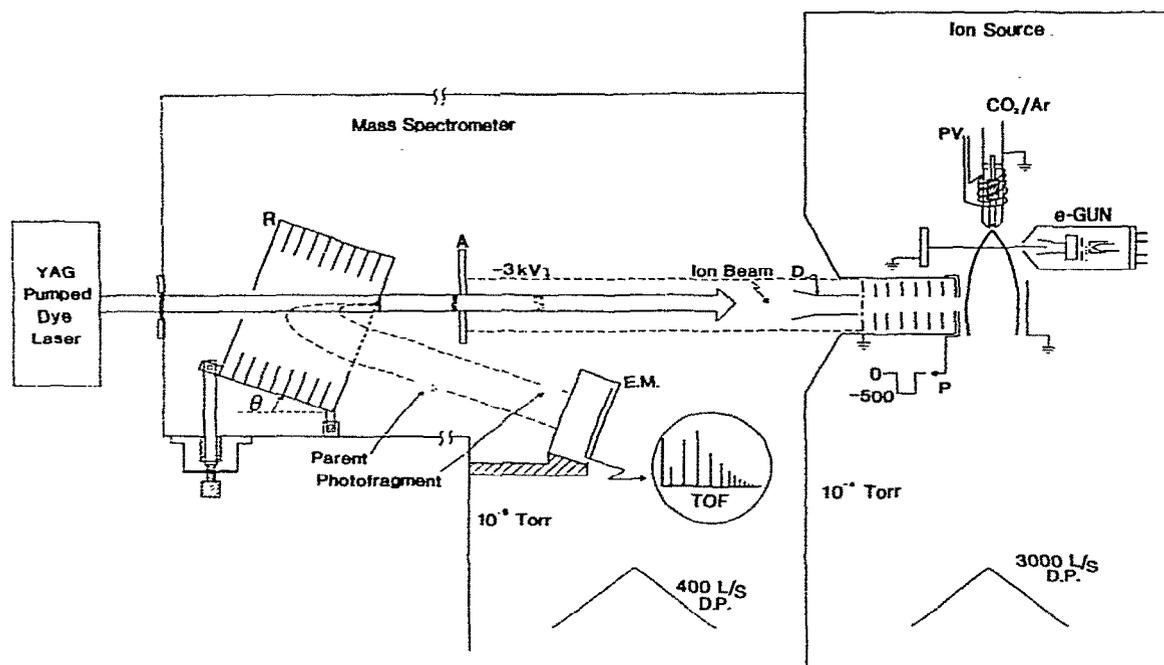
Fig. 1. Schematic diagram of apparatus. PV, pulsed valve (Bosch); P, pulsed extraction plate; DP, diffusion pump; D, deflectors; R, "reflectron" field; A, 9 mm aperture; E.M., Johnston electron multiplier; TOF, time-of-flicht spectrum, $\theta = 10°$. The spatial focusing of the first mass spectrometer is illustrated by bunching of the ion beam. The separation of parents from photofragment daughters is similarly indicated along with schematic trajectories.

spectra thus have as a time origin the rapid switching of the draw-out voltage, *nor* the usual laser-pulse-initiated TOF spectra where the ions are created in a constant field region. The clusters are photodissociated during the free flight by passing a pulsed laser beam down the axis of the flight tube. Parent ions are separated from daughters by reflecting electric field, and are detected with an electron mulitiplier after another short free-flight region. This arrangement is capable of resolving the daughter masses as well as isolating parents [10], but the work reported in this paper only involves observation of parent photodestruction.

The performance of this cluster ion source is illustrated in fig. 2, showing the variation of the $(CO_2)_n^+$ time-of-flight spectra with the distance between the electron beam (200 eV energy, 100 μA, 1 mm diameter) and the nozzle. Fig. 2a results from a distance of 2.8 cm, and only shows a peak from the CO_2^+ monomer. Thus. in the absence of subsequent collisions, the primary ion produced by electron impact is the

monomer, with very little contribution to higher clusters from the ionization of neutral clusters formed in the jet. In fact, our previous work on the jet-cooled, microwave—optical double resonance of ions [11] employed the same apparatus to generate an intense beam of rotationally cold (15 K) CO^+ monomers. This absence of neutral clusters is not surprising since the expansion conditions are quite mild (1.5 atm backing pressure with a 1.0 mm diameter nozzle at room temperature) and do not favor extensive clustering of the neutrals.

The degree of clustering increases dramatically as the electron beam is moved toward the nozzle, as shown in figs. 2b—2d. Higher clusters are successively formed until, at 0.2 cm distance (fig. 2d) a distribution peaking at $n = 8$ and continuing out to about 17 is readily obtained. The pulsed molecular beam density at this distance is about $10^{17}/cm^3$, sufficiently high that three-body clustering rates [12] are a significant loss mechanism for the nascent CO_2^+ species formed
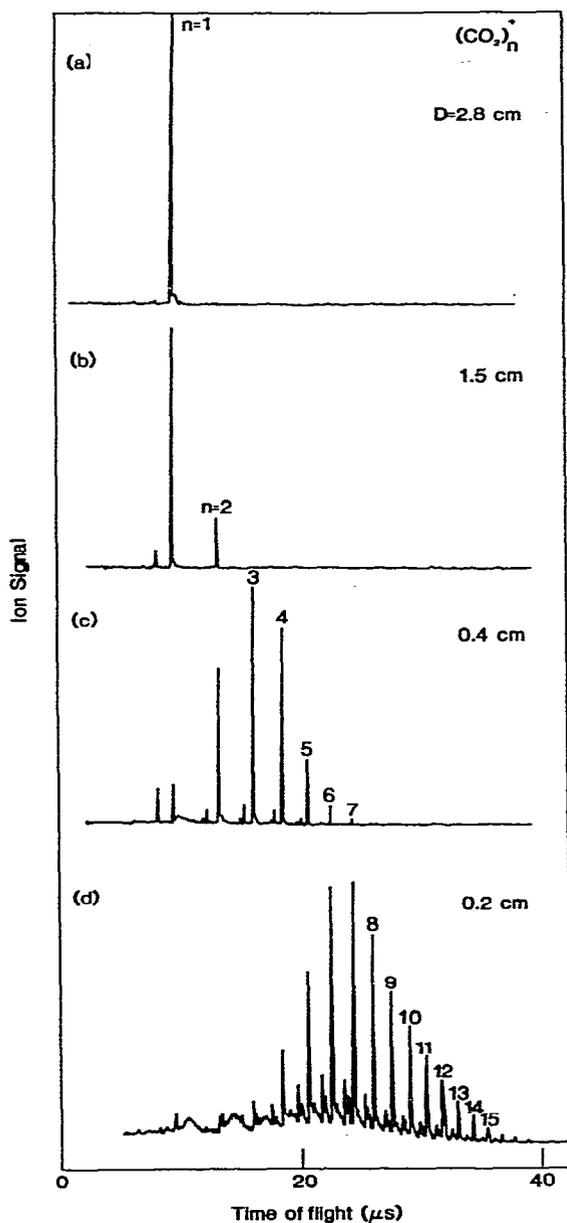
Fig. 2. TOF mass spectra from the nucleation cluster source as the distance from the electron beam to the nozzle is varied. Clusters result from successive attachment of CO_2 to CO_2^+, not from ionization of neutral CO_2 clusters.

by electron impact. At such high neutral densities, the ion—neutral vibrational-relaxation rates are quite high [13], resulting in cluster ions at least partially cooled to the ambient (≈ 20 K) temperature of the jet. Additionally, the traces in figs. 2c and 2d display new peaks between those corresponding to $(CO_2)_n^+$, some of which are sharp (as between $n = 7$ and 8), and some which are broad (as between $n = 1, 2$ and 3). The sharp features correspond to $(CO_2)_n^+$ with added O_2 or H_2), and are due to impurities in the gas handling system. The broad peaks arise from collision-induced dissociation of the higher clusters during the extraction from the high-density jet, yielding $n = 1, 2$ and 3 fragment ions.

The time-of-flight (TOF) spectrometer used here is a hybrid of the spatial-focusing Wiley—Mclaren [14] type and the reflectron type developed by Mamyrin et al. [15] and used recently by Boesl et al. [10] in their laser multiphoton ionization studies. A similar apparatus has also been used very recently by Echt et al. [16] in a study of collision-induced dissociation of ammonia cluster ions. Unlike the laser ionization experiments, however, the spatial distribution of cluster ions in the nucleation source is quite broad (≈ 25 cm^2 corss section ion cloud) after they have drifted 10 cm down in the molecular beam. The extraction plates are spaced 5 cm apart to avoid both perturbation of the supersonic flow and collision-induced dissociation from pulsed extraction in a high-density region. The extraction plates are pulsed at 500 V (20 ns risetime), resulting in a high ion collection efficiency, but also introducing a rather large (500 eV) energy spread in the ion beam. Even so, good mass resolution can be maintained by spatially focusing the parent clusters 1.3 m from the source. This focus is achieved by a second 2500 V, 5 cm long acceleration region just after the pulse-out plates. This time focusing of the parent ions yields a mass resolution of the parent ions of about $M/\Delta M = 120$ at 2500 V energy, in spite of the 20% energy spread in the ion beam. The flight tube is differentially pumped through a 3 mm aperture on the pulse-out plate and held at about 1×10^{-6} Torr. At this pressure, collision-induced dissociation is not a major process.

Parent cluster ions are isolated from the photodissociated daughter ions in the second stage of our TOF spectrometer, using a constant retarding field ("reflec-

tron") [15] which reverses the direction of the ions, followed by a short additional free-flight region of 20 cm before detection. Separation of parents from daughters is slightly complicated by the 20% energy spread of the parent beam. Thus, an energy analyzer type of mass filter results in modest mass resolution ($M/\Delta M \approx 5$) between parents and daughters. With the reflectron approach, the ion trajectories are not resolved and, although the trajectories of parents and daughters are distinct, the angle of the reflecting field ($\approx 10°$) is such that all masses are detected on the large surface area (1.5" diameter) of the Johnston electron multiplier. The arrival times of the ions are bunched about each mass, yielding a secondary TOF spectrum, originating at the parent peak and extending to shorter times. This secondary spectrum contains the fragmentation pattern of the parent at a resolution $M/\Delta M$ of about 50. Schematic trajectories are indicated in fig. 1.

Photofragmentation takes place during the 1.3 m free flight of the parent ions with the laser collinear with respect to the ion beam. Measurement of relative photodissociation cross sections requires some care to ensure that the overlap of the beams is constant for all clusters. These geometrical parameters were controlled by adjustment of the timing between firing the laser and pulsing out the ions, and careful adjustment of the mass-dependent ion trajectories to maximize photodissociation for each cluster. TOF spectra were recorded with a 10 ns/channel transient recorder (Transiac) and 200 laser on—laser off cycles were averaged to yield the photodestruction ratio ($I_{off} - I_{on})/I_{off}$, where I indicates the integral of the TOF peak for a particular cluster.

Laser energies were 2 to 20 mJ/pulse, and the energy used in a particular situation was chosen to obtain about 20% photodestruction. Power dependence studies showed that multiphoton absorption was unimportant and that this degree of attenuation corresponded to a linear regime. The high power limit of destruction occurred at 50 to 80% depletion. Where different cluster ions had radically different photodestruction cross sections, such as at 1064 nm, the power dependence of the fraction of ions depleted showed that the smaller cross-section species had the same saturation limit as the larger, indicating that the cross-section differences are real and not due to factors such as isomers in the beam or variation in beam overlap. To test the performance of this instrument, the

relative photodestruction cross sections for $(NO)_2^+$ and $(NO)_3^+$ were measured at 532 nm, in order to compare with recent measurements by Jarrold et al. [6]. Our value of 4.7 (0.6) for the ($n = 3/n = 2$) ratio compares with the reported value of 4.3 (0.3).

3. Results and discussion

Relative photodestruction cross sections for $(CO_2)_n^+$ with $n = 2-10$ are shown in fig. 3, normalized to $n = 2$. It is striking that *all* clusters measured at these wavelengths (1064, 644 and 532 nm) have a significant cross section; in fact, almost *identical* cross sections are found at 532 nm. The CO_2^+ and CO_2 monomers, with their first electronically excited states lying at 3500 Å [17] and 2200 Å [18] respectively, do not absorb in the visible. The dimer ion does absorb here, however, and photodestruction measurements have been carried out from 8000 to 4000 Å [8]. The absorption is bell shaped, peaking at about 650 nm, with about one-fourth of the maximum cross section at 1064 and 532 nm. This band appears due to excitation to a potential curve strongly repulsive between the CO_2 centers, and involves bonding electrons of the dimer ion ($D_0 = 11.8$ kcal/mol) [19]. The dimer spectrum is quite similar to bound—free spectra of diatomic molecules, where excitation of a stable ground state to a repulsive state arises in a broad absorption spectrum governed by Franck—Condon overlap or the "reflection" principle [20]. For such spectra, the high- and low-energy wings of the absorption profile are determined by the inner and outer turning points of the ground-state wavefunction and the steepness of the repulsive curve. It is therefore significant that the higher clusters absorb very similarly to the dimer. Such a situation is not universal, as recent measurements of the $(NO)_2^+$ and $(NO)_3^+$ photodestruction cross sections show [6] that the dimer and trimer are quite different. The behavior of higher clusters is not presently known. In the case of the CO_2-based ion clusters, it seems that the dimer ion species is the major carrier of oscillator strength in the visible region.

While the overall nature of the absorption of the CO_2 ion clusters follows the behavior of the dimer, fig. 3 does show that there are quantitative differences. At 644 nm, there is a gradual increase in cross section with n, while at 1064 nm the cross section falls off
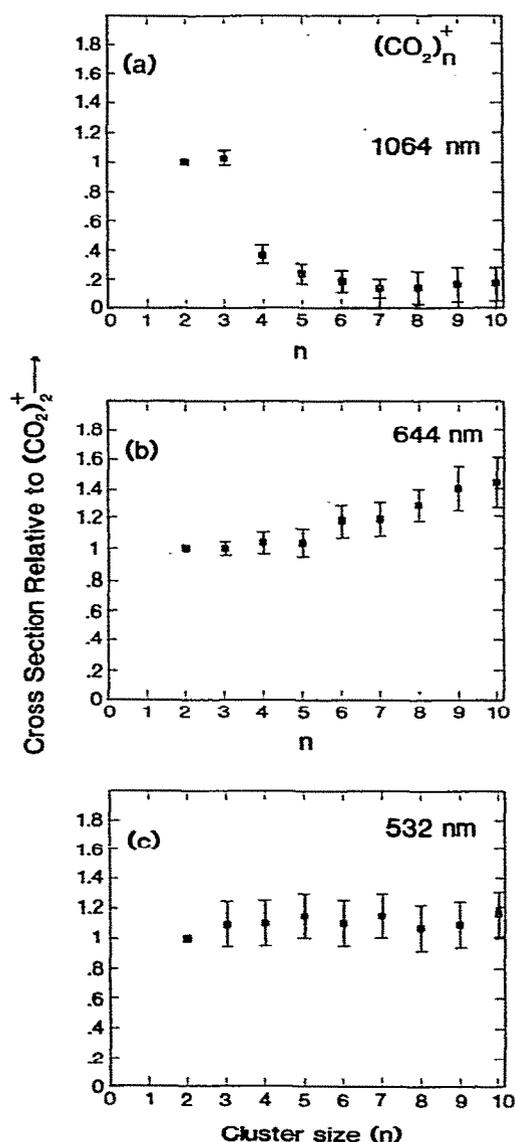
Fig. 3. Photodestruction cross sections for $(CO_2)_n^+$ relative to $n = 2$ at (a) 1064 nm, (b) 644 nm and (c) 532 nm.

rapidly at $n = 4$ and stays low out to at least $n = 10$.

Since this experiment is sensitive only to species for which absorption of a photon leads to fragmentation on the timescale of the experiment, the observed cross sections are a convolution of the absorption probability of the cluster at a given wavelength and the dy-

namical probability that the cluster falls apart with the internal energy imparted to it by the photon. This is relevant to the interpretation of the cross-section data in fig. 3, since the lower cross-section data at 1064 nm could result from smaller unimolecular rates at this, the smallest photon energy investigated. Qualitatively, this seems reasonable since the larger clusters should have decreased unimolecular decay rates. Quantitatively, however, the fall-off of the cross section stops at $n = 5$, whereas one would expect this trend to continue if the unimolecular decomposition model were correct. Further, there was no difference in the relative cross sections at 1064 nm when the ions were photodissociated either at the beginning or the end of the flight tube. Unimolecular behavior is thus not evident on a 3 to 25 μs timescale. Finally, metastable peaks were not found when the ions were photodissociated inside the reflectron, eliminating the possiblity of unimolecular decay on the 0.5 to 2 μs timescale. We therefore seek an explanation of the data in fig. 3 involving the absorption process.

Since each clusters' absorption spectrum is similar to the dimer spectrum, and since dimer absorption leads to prompt breaking of the dimer bond, we interpret the higher cluster spectra by initial absorption into a $(CO_2)_2^+$ chromophore, followed by dissociation of the dimer. Additionally, the $CO_2 \cdot (CO_2)_n^+$ binding energy was found to drop drastically from $n = 1$ to 2 (11.8 versus 3.3 kcal/mole), but remain nearly constant from $n = 2$ to 3 (3.3 versus 2.8 kcal/mole) [19], supporting the model of a charged dimer within a neutral cluster. Such behavior of nucleation about an ion cluster has been shown in calculations on $(H_n)^+$ [21], where the structure is found to be best described as $(H_3)^+ \cdot (H_2)_m$. For CO_2, this model degrades the photon energy into the repulsive motion of the molecular centers, leading to dissociation of the cluster. We observe that, at the high-energy tail (532 nm) of the dimer spectrum, all of the clusters have the same cross section. Since the dimer absorption here is largely determined by overlap at short CO_2–CO_2 distance [8], we conclude that the inner turning point on the dimer excited state repulsive curve is not affected significantly by further clustering.

The long-wavelength portion of the cross section is, however, strongly dependent on cluster size and, in this model, the environment of the dimer chromophore. The low-energy tail of the absorption spectrum results

from the behavior of the repulsive and bound potential curves at large intermolecular distance, that portion most likely to be distorted by clustering. If the dissociation limit of the repulsive curve were raised owing to solvation of the CO_2^+ fragment by the rest of the cluster, a decrease in cross section at 1064 nm would result. Moreover, the constant cross section at $n > 5$ at this wavelength would indicate that the local environment of the dimer had stabilized, with further clustering having minimal impact on the dimer fragmentation event. Alternatively, the 1064 nm drop-off could be interpreted as due to changes solely in the ground-state dimer wavefunction owing to clustering about it, such that the large intermolecular distance portion of the wavefunction is attenuated by the presence of additional CO_2 molecules. In any event, the wavelength data are consistent with a constant integrated absorption model with slight changes in the shape of the long-wavelength portion of the absorption spectrum.

In summary, we have constructed an apparatus that is capable of measuring mass-selected cluster ion photoabsorption up to at least 10–20 monomers. The data show clearly the role of the $CO_2^+ \cdot CO_2$ chromophore in photoabsorption. The measurement of the fragmentation spectra from the mass-selected clusters will be of great importance in understanding the cluster ion photophysics and is currently in progress in our laboratory.

Acknowledgement

References

[1] T.D. Märk and A.W. Castleman Jr., in: Advances in atomic and molecular physics, Vol. 20, eds. D.R. Bates and B. Bederson (Academic Press, New York, 1984), to be published.

[2] R.J. Beuhler and L. Friedman, J. Chem. Phys. 77 (1982) 2549.

[3] V. Hermann, B.D. Kay and A.W. Castleman Jr., Chem. Phys. 72 (1982) 185.

[4] O. Echt, K. Sattler and E. Recknagel, Phys. Letters 90A (1982) 185

[5] D.E. Hunton, M. Hofmann, T.G. Lindeman, C.R. Albertoni and A.W. Castleman Jr., J. Chem. Phys., submitted for publication.

[6] M.F. Jarrold, A.J. Illies and M.T. Bowers, J. Chem. Phys. 81 (1984) 222.

[7] J.Q. Searcy and J.B. Fenn, J. Chem. Phys. 61 (1974) 5282.

[8] G.P. Smith and L.C. Lee, J. Chem. Phys. 69 (1978) 5393.

[9] A.J. Stace, J. Phys. Chem. 87 (1983) 2286.

[10] U. Boesl, H.J. Neusser, R. Weinkauf and E.W. Schlag, J. Phys. Chem. 86 (1982) 4857.

[11] M.A. Johnson, M.L. Alexander, I. Hertel and W.C. Lineberger, Chem. Phys. Letters 105 (1984) 374.

[12] P.A.M. van Koppen, M.F. Jarrold, M.T. Bowers, L.M. Bass and K.R. Jennings, J. Chem. Phys. 81 (1984) 288.

[13] H. Böhringer, M. Durup-Ferguson, D.W. Fahey, F.C. Fehsenfeld and E.E. Ferguson, J. Chem. Phys. 79 (1983) 4201.

[14] W.C. Wiley and I.H. Mclaren, Rev. Sci. Instr. 26 (1955) 1150.

[15] B.A. Mamyrin, V.I. Karataev, D.V. Shmikk and V.A. Zagulin, Soviet Phys. JETP 37 (1973) 45.

[16] O. Echt, P.D. Dao, S. Morgan and A.W. Castleman, Jr., J. Chem. Phys., submitted for publication.

[17] D. Gauyacq, C. Larcher and J. Rostas, Can. J. Phys. 57 (1979) 1634.

[18] G. Herzberg, Electronic spectra of polyatomic molecules (Van Nostrand, Princeton, 1966).

[19] S.H. Linn and C.Y. Ng, J. Chem. Phys. 75 (1981) 4921.

[20] G. Herzberg, Spectra of diatomic molecules, 2nd Ed. (Van Nostrand, Princeton, 1950) p. 393.

[21] Y. Yamaguchi, J.F. Gaw and H.F. Schaefer III, J. Chem. Phys. 78 (1983) 4074.